Endocrine (2012) 42:39–51
DOI 10.1007/s12020-012-9691-2

REVIEW

New advances in imaging osteoporosis and its complications

James F. Griffith · Harry K. Genant

Received: 7 February 2012 / Accepted: 30 April 2012 / Published online: 23 May 2012

Abstract Tremendous advances have been made over the past several decades in assessing osteoporosis and its complications. High resolution imaging combined with sophisticated computational techniques now provide a detailed analysis of bone structure and a much more accurate prediction of bone strength. These techniques have shown how different mechanisms of age-related bone weakening exist in males and females. Limitations peculiar to these more advanced imaging techniques currently hinder their adoption into mainstream clinical practice. As such, the ultimate quest remains a readily available, safe, high resolution technique capable of fully predicting bone strength, capable of showing how bone strength is faltering and precisely monitoring treatment effect. Whether this technique will be based on acquisition of spine/hip data or data obtained at peripheral sites reflective of changes happening in the spine and hip regions is still not clear. In the meantime, mainstream imaging will continue to improve the detection of osteoporosis related insufficiency fracture in the clinical setting. We, as clinicians, should aim to increase awareness of this fracture type both as a frequent and varied source of pain in patients with osteoporosis and as the ultimate marker of severely impaired bone strength.

Keywords Osteoporosis · Fracture · Imaging · DXA · Computed tomography · Magnetic resonance imaging

J. F. Griffith (✉)
Department of Imaging and Interventional Radiology, The Chinese University of Hong Kong, Shatin, Hong Kong
e-mail: griffith@cuhk.edu.hk

H. K. Genant
University of California, San Francisco, CA, USA

Introduction

It is fortuitous that as the prevalence of osteoporosis has increased over the past 30 years, there has been a parallel increase in the range and capability of imaging modalities used to evaluate osteoporosis and its complications. These advances in medical imaging and data processing have improved understanding of the osteoporotic process as well as bone anatomy, physiology, and pathology in a broader sense. Much has been learnt regarding the diagnosis and assessment of osteoporosis as well as limitations of current evaluation methods. Current techniques based on density measurement, in many respects, diagnose osteoporosis too late with bone strength being significantly weakened before density criteria are met. Even with appropriate treatment at this stage, bone strength will not return to normal. Although practical limitations such as machine cost, clinical usage, and radiation issues limit adoption of these newer imaging applications into everyday clinical practice, they are nevertheless very much at the forefront with regard to bone quality research and the assessment of new osteoporotic treatments [1, 2].

The same practical limitations do not apply to evaluating the main complication of osteoporosis, namely insufficiency fracture. Modern imaging modalities have enabled recognition and evaluation of insufficiency fracture to a high level of accuracy significantly impacting day-to-day clinical practice and improving patient wellbeing. This review addresses recent imaging advances in the diagnosis and assessment of osteoporosis focusing primarily on new information gaining regarding the pathogenesis of osteoporotic insufficiency fracture. Second, we discuss advances in imaging with regard to recognition and characterization of insufficiency fracture.

Advances in imaging osteoporosis

Dual X-ray absorptiometry (DXA)

Since DXA first came into clinical practice in the mid-1980s, it has become widely applied as a means to diagnose and monitor osteoporosis. In 1994, the WHO recommended DXA-based thresholds for normal bone density (*T*-score >1.0), osteopenia (*T*-score <1.0 and >2.5), and osteoporosis (*T*-score >2.5) [3]. DXA examination measures areal bone mineral density (BMD) in g/cm^2. Areal densitometry has limitations particularly in the spine. For example, vertebral body depth is not taken into account such that larger (i.e., deeper) vertebrae in men or growing children appear spuriously more dense than smaller (i.e., less deep) vertebrae. Similarly, areal projectional techniques cannot separate cortical and trabecular bone density and cannot compensate for features such as scoliosis, marginal osteophytosis, facet joint arthrosis or vascular calcification all of which tend to erroneously increase densitometric measurement. As a result of these and other confounding factors, lumbar spine BMD tends to remain static or even increase in post-menopausal women [4]. On the other hand, increased body fat as well as increased marrow fat may spuriously decrease DXA lumbar spine and hip measurements more so than other densitometry techniques [5, 6]. Nevertheless, despite these limitations, BMD measurement by DXA is the best available surrogate marker of osteoporosis. The lower the BMD, the greater the risk of sustaining an insufficiency fracture [7] with fracture risk increasing approximately 1.5-fold for every SD (i.e., *T*-score) age-adjusted reduction in BMD. Similarly, the lower the BMD, the more likely the patient is to benefit from osteoporotic medication [8].

However, osteoporosis is not solely a disease of reduced BMD as exemplified in the WHO position which defines osteoporosis as a skeletal disease characterized not just by "low bone mass" but also by "micro-architectural deterioration of bone" [WHO 1995]. A more encompassing consideration is to think of osteoporosis as a disease of reduced bone strength [9]. Bone strength is the ability of bone to resist fracture and depends on bone quality as well as bone density. Bone qualify represents all aspects of bone strength other than bone density and incorporates such wide ranging features as bone macrostructure, microstructure, mineralization, microdamage, and collagen status. The limitation of using BMD as the sole determinant of bone strength has been borne out by many studies. For example, nearly half of all post-menopausal women who sustained an insufficiency fracture over a 9-year period, had a baseline BMD in the osteopenic range while one-tenth had normal baseline BMD [10]. In another study, nearly half of all non-vertebral fractures occurred in women who did not have osteoporosis based on DXA examination [11]. A similar discrepancy was seen in patients treated with anti-resorptive therapy, in that the 5–8 % improvement in BMD did not explain the observed 50–60 % decrease in fracture incidence [12, 13]. This latter discrepancy reflects the positive effect that osteoporotic medication has on bone quality to improve bone strength over and above the effect of increasing BMD. It would clearly be advantageous if DXA could provide additional information on bone quality in addition to BMD. With this in mind, the potential of standard DXA examination have been enhanced by simultaneous vertebral fracture assessment (VFA) by DXA as well as incorporating geometric elements based on additional analysis of two- or three-dimensional DXA images.

DXA systems equipped with in-built fan beam technology and supportive software can acquire diagnostic quality images of the lower thoracic and lumbar spines enabling VFA of the T7 to L4 vertebrae. VFA by DXA can be performed at the same time as bone densitometry with obvious cost and practical advantages over spinal radiography. Although image resolution is modest compared to radiography, it is still adequate to detect most vertebral fractures [14]. VFA has high sensitivity for diagnosing moderate to severe vertebral fractures and moderate sensitivity for mild vertebral fractures (Fig. 1). VFA, in allowing recognition of unsuspected vertebral fracture, provides bone strength information over and above BMD. This additional information can be incorporated into the fracture risk assessment (FRAX) model along with clinical risk factors to improve 10-year prediction of major osteoporotic fracture [15].

For the hip region, advances in DXA software allows automatic calculation of several proximal femoral structural parameters (such as hip axis length, cross-sectional moment of inertia, femoral neck shaft angle, and femoral neck width) along with areal BMD. These structural parameters can be combined with body size to calculate composite femoral strength indices for different failure modes (compression, bending, and impact) [16, 17] significantly improving hip fracture risk prediction compared to *T*-score alone [18]. For example, despite having higher femoral neck BMD, diabetic women were found to have lower composite femoral strength indices consistent with their known higher hip fracture risk [19]. Similarly, Chinese subjects, even though their lower femoral neck BMD was lower, were found to have a higher femoral compressive strength index than Caucasians which helps explain their lower incidence of hip fractures [17].

Geometric data are best obtained from volumetric three-dimensional data, rather than the two-dimensional DXA data and with this in mind, the feasibility of volumetric X-ray absorptiometry (VXA) has been studied [20].

Fig. 1 Lateral (**a**) and frontal (**b**) VFA by DXA showing moderate fracture of L1 vertebral body (*arrows*)

Combining areal BMD with VXA-derived 3D geometric parameters (such as femoral head diameter and mid-femoral neck cross-sectional area) improves failure load prediction over BMD measurement [21]. VXA shows excellent correlation with volumetric quantitative CT (vQCT) structural (femoral neck axis length, cross-sectional area) and density parameters [22]. Although VXA cannot currently distinguish between the cortical and trabecular bone components and cannot determine cortical thickness, it shows promise as a low cost, low radiation, clinically applicable technique predictive of proximal femoral strength. However, its ability to improve prediction of proximal femoral fracture in clinical studies has not yet been reported.

Advances in DXA hardware and analytical techniques now enable DXA to measure even relatively small changes in body composition and aortic calcification [23, 24]. The amount of fat (g), lean mass (g), and % fat for the arm, trunk, leg or total body can be measured with good precision [23]. This is clearly useful if studying the relationship between osteoporosis and associated conditions such as sacropenia, aging, obesity, thinness, anorexia, metabolic syndrome, diabetes, and cardiovascular disease. [23]. Modern DXA scanners also compare favorably with radiography in detecting and grading aortic calcification, a known associate of osteoporosis and significant cardiovascular risk factor [24, 25].

Computed tomography (CT)

Many of the limitations of areal DXA measurement can be overcome by multidetector CT which allows higher spatial resolution, improved delineation of bone architecture, and acquisition of near isotropic vQCT datasets [26]. Volumetric QCT data correlate highly ($r = 0.92$, $p < 0.0001$) with reference standards for bone volume fraction (BV/TV) and trabecular spacing though, as expected, fares less well with trabecular thickness and number, as the spatial resolution of multidetector (500 μm) is larger than average trabecular thickness of 50–150 μm and more comparable to average trabecular spacing of 200–2,000 μm [26] Bone is an architecturally adaptive tissue which responds to mechanical load and use. Gender differences in fracture rates are not explained by differences in areal BMD [27]. Males have larger bones than females, which are also substantially more heavily loaded [28]. QCT-based studies have demonstrated how aging Caucasian men loose similar amounts of bone to Caucasian women from the endosteal cortical surface. However, net bone loss is less in men as endosteal bone loss is offset by increased bone deposition on the periosteal surface. The greater propensity of men over women to deposit bone in the periosteal areas helps them increase bone cross-sectional area, maintain bone strength, and reduce vertebral fracture risk compared to women [29, 30].

A vertebral fracture occurs when the loading applied to a vertebral body exceed its strength. Functional loading of the spine is primarily compressive. Most vertebral fractures occur in the mid-thoracic and thoracolumbar regions, often in incremental or stepwise fashion with severity varying from a minor endplate fracture to a complete vertebral body fracture. [31]. Compressive loading is accentuated in the mid-thoracic spine during flexion and in the thoracolumbar region between the relatively fixed thoracic and more mobile lumbar spine. The weakest parts of the vertebral body seem to be the central areas of the endplates and the anterosuperior aspect of the vertebral body where lower bone mass is not compensated by higher structural strength [32]. Fracture of a single vertebral body, particularly of anterior wedge type, shifts compressive forces toward the anterior aspects of the vertebral bodies to the extent that a "vertebral fracture cascade" may ensue, with fractures in adjacent vertebrae occurring in quite rapid succession [33].

Micro-CT, combined with finite element analysis (FEA), have shown that major load pathways through the

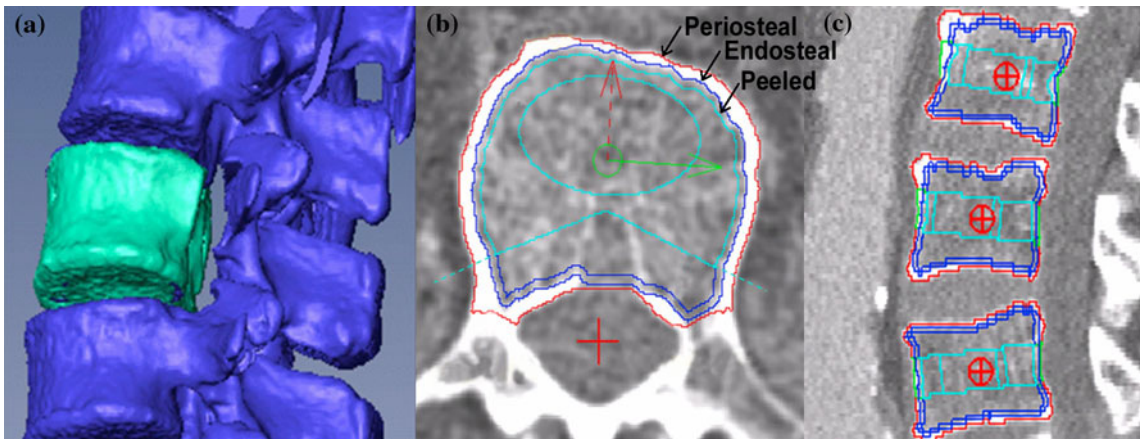

Fig. 2 **a** Volumetric QCT of lumbar spine with automated anatomical coordinates outlining **b** the periosteal, endosteal, and juxta-endosteal ("peeled") contours of the vertebral body. Several different VOI's can be evaluated such as the total VOI, trabecular VOI, peeled, elliptical, and Pacman VOIs in the axial plane as well as **c** the superior, mid-vertebral, and inferior VOI's in the sagittal plane. (Courtesy of Klaus Engelke)

vertebral body seem to parallel the vertical trabeculae. The cortical shell and the horizontal trabeculae, although important in bracing vertical trabeculae against buckling, seem to have only a modest role in resisting compressive forces [34]. Although all trabeculae reduce in number and tend to become more rod-like than plate-like with increasing age, only the horizontal trabeculae reduce in thickness [35, 36], possibly due to horizontal trabeculae being reabsorbed preferentially as the result of "adaptive strain resorption," while vertical trabeculae are reabsorbed as a result of microdamage [37].

While density and geometric parameters enable prediction of vertebral strength, a more direct measurement of bone strength is provided by combining QCT with FEA. Mechanical properties are assigned to each finite element of high resolution CT (or MRI) model following segmentation and decomposition to provide information on parameters such as stiffness, estimated load failure, and stress distribution [38]. One can simulate physiological loading patterns with compressive loading being applied for the spine and lateral loading simulating a sideways fall for the hip (Fig. 2). FEA of vQCT data has shown how vertebral body strength decreases with age twice as much in women than men and that this sex difference is primarily due to a greater decline in cortical bone strength in women over and above the decline in trabecular bone strength which is similar for both sexes [39].

While vertebral fracture are usually the first osteoporotic fracture to occur and the source of considerable pain, immobility and poor self image, the impact of proximal femoral insufficiency fracture with regard to morbidity, mortality and cost is greater. About two-thirds of hip fractures occur in females. Age-related bone loss results in proximal femoral cortical thickness in elderly females being only about one-half that of middle-aged women while trabecular volumetric BMD is only about one-third [40]. In addition to progressive bones loss which is not that dissimilar for both sexes, women are at increased risk of femoral neck fracture by having smaller femoral necks; tending to loose trabecular number and connectivity (as opposed to men who sustain trabecular thinning); and have a lower propensity than men for bone deposition on the periosteal side of the cortex. Although females have slightly thicker anteroinferior femoral cortices than males, males have a higher femoral neck bending strength making them less susceptible to fracture [41]. Similar differences in proximal femoral bone architecture help account for observed inter-racial differences in hip fracture risk [40].

FEA studies of the proximal femur provide more insight. In an age-stratified cohort of over 600 men and women, FEA of QCT data showed how lifetime reduction in proximal femoral strength (↓ 65 % women, ↓ 39 % men) was much greater than reduction in femoral neck areal BMD (↓ 26 % women, ↓ 21 % men). This decline in bone strength starts about 10 years earlier (i.e., in the mid-1940s) in women than men. This early onset had a greater effect on the eventual decline in femoral strength than peak bone mass or annual rates of bone loss. For FEA, a proximal femoral strength of <3,000 N has been suggested as being representative of "low femoral strength." And this <3,000 N threshold is also that most predictive of insufficiency fractures outside the hip [42]. "Low femoral strength" is seen to more common in the elderly than traditional DXA-based measures of osteoporosis [43].

Structural parameters obtained by MDCT provide a better discriminator of treatment change than DXA and may be evident as early as 12 months post-baseline. For example, in post-menopausal women teriparatide increased

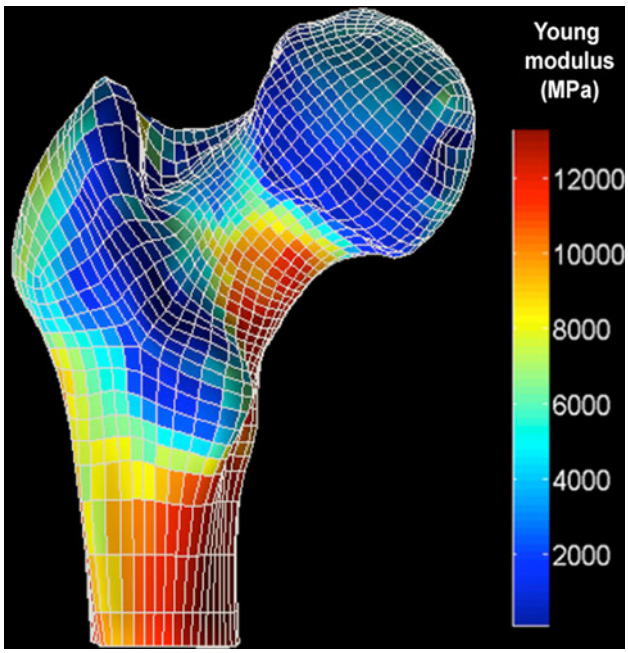

Fig. 3 Volumetric QCT provides a basis for FEA of the proximal femur. Note how stress distribution in the proximal femur as related to color coding is greatest along the inferomedial aspect of the femoral neck and proximal shaft (Courtesy of Klaus Engelke)

vertebral apparent bone volume fraction (app. BV/TV) by 30.6 ± 4.4 % (mean ± SE), and apparent trabecular number (app. Tb.N.) by 19.0 ± 3.2 % compared to a 6.4 ± 0.7 % increase in DXA-derived areal BMD with significant changes in these variables detectable by QCT at 6 months post-baseline [44]. Improvement in bone strength with medication is related to both the location of structural change as well as the degree of structural change. Automated anatomical coordinate systems, such as medical image analysis framework (MIAF), allow one to appreciate how geometric parameters and treatment affect trabecular and cortical bone and the contribution to bone strength [45, 46]. For example, 1 year of ibandronate treatment led to increased volumetric density in the subcortical and extended trabecular areas of the proximal femur as well as the extended cortical and superior/inferior trabecular regions of the vertebral body (Fig. 3), all of which are mechanically significant areas [47].

High resolution peripheral quantitative CT (HR-pQCT)

The main limitations of volumetric CT are cost, clinical accessibility, and radiation dose. It would be helpful if a more dedicated peripheral CT unit could provide images of high resolution at lower cost and lower radiation dose, particularly if these peripheral parameters of bone quality were shown to mirror those occurring more centrally in the vertebrae or proximal femora. Such a HR-pQCT (Xtreme CT, Scanco Medical AG, Basserdorf, Switzerland) has become available allowing much higher resolution images than standard peripheral QCT systems. HR-pQCT can examine the distal radius or distal tibia in 2.8 min acquiring a tack of 110 images over a 9 mm length with a nominal isotropic voxel size of ~90 μm (Fig. 4). Structural parameters acquired are trabecular number, thickness, separation, structure model index, connectivity, anisotropy, and cortical thickness with all structural parameters derived from density measurements assuming a fixed mineralization of 1,200 mg HA/cm^3. Limitations of HR-pQCT are movement artifact, particularly of the radius, and confinement of imaging to the ultradistal radius or tibia. Although

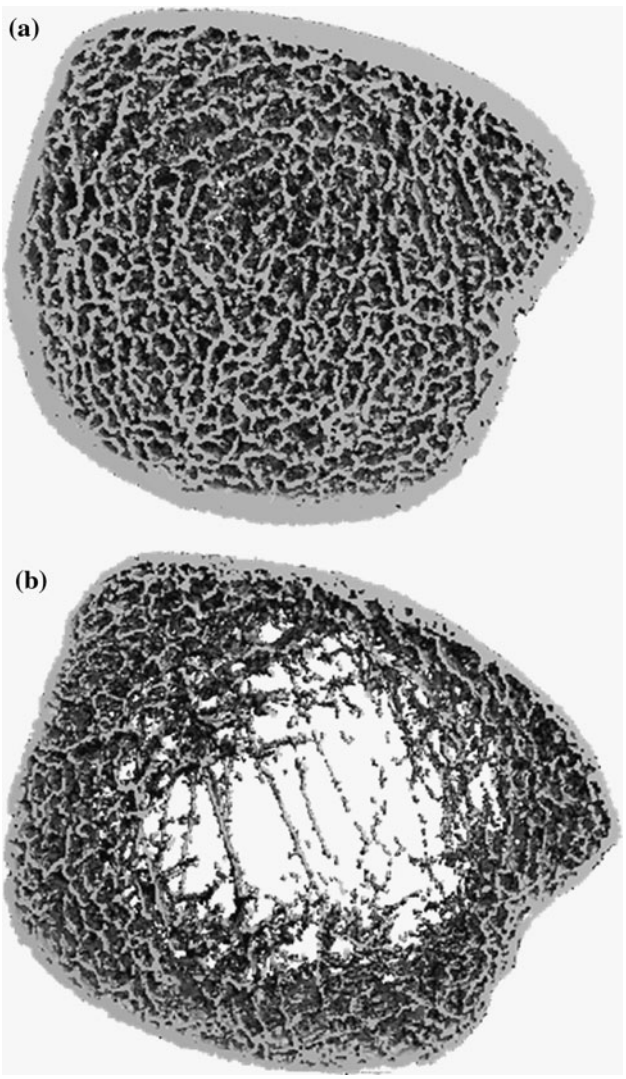

Fig. 4 High resolution peripheral CT (Xtreme CT) of distal tibia in subject with **a** normal BMD and **b** severe osteoporosis. The deterioration in trabecular architecture with reduced trabecular number, trabecular thinning, increased trabecular spacing as well as generalized cortical thinning and increased cortical porosity is readily appreciable in the osteoporotic subject

the analysis programs for structural data are density-based, and as such will strongly correlate with vBMD, the structural parameters obtained by HR-pQCT compare well with those obtained by microCT. Good correlation ($r = 0.50$–0.78) was also found between density and stiffness parameters obtained peripherally by HR-pQCT and centrally by vQCT [48].

Cross-sectional high resolution pQCT study has shown how men have thicker trabeculae and tend to undergo trabecular thinning rather than loss at the distal radius with aging as opposed to women who tend to lose trabeculae with an increase in trabecular spacing [49]. This enhances information from standard peripheral QCT-based studies showing how both sexes start to loss appendicular trabecular bone in early adulthood with cortical bone loss occurring later though considerably earlier in females than males [50]. As decrease in trabecular number impacts bone strength more than a decrease in thickness and as the distal radial strength is quite cortical dependent, these studies can help explain the higher distal radial fracture rate in elderly females.

HR-pQCT techniques can be used to discriminate the treatment effect of anti-resorptive agents with different mechanisms of action [51]. For example, in a double blind study, denosumab, a fully human monoclonal antibody to Rank ligand (RANKL), prevented expected decline cortical and trabecular BMD at the distal radius and tibia more than alendronate ($p < 0.024$) and led to a greater improvement in polar moment of inertia [51].

Magnetic resonance imaging (MRI)

MRI has several advantages over CT in assessing bone quality. It does not use ionizing radiation; it can obtain image data directly in any orthogonal plane and has the ability to investigate physiological aspects of bone such as marrow fat content, marrow diffusion, marrow perfusion, and water content. Its disadvantages, however, include cost, resolution issues, considerable time requirement, and more technically demanding data acquisition and analysis.

High resolution MR imaging of the central skeleton is limited by signal to noise ratio (SNR) and resolution issues aggravated by the persistence of hematopoietic marrow in the axial skeleton as this contrasts less well with adjacent trabeculae than marrow fat. Therefore, most in vivo MR studies have addressed relatively superficial peripheral sites such as the distal radius, distal tibia, and calcaneus as these trabecular-rich areas are accessible to small high resolution coils. Nearly all MR-derived structural parameters of the distal radius are better than DXA at differentiating women with and without vertebral fracture [52].

However, with pulse sequence and coil optimization, the proximal femur can be accessible for bone quality analysis with high resolution images of the proximal femur achievable with an in-plane resolution of 254 μm and a minimal slice thickness of 500 μm [53, 54]. MRI of the distal radius and inter-trochanteric proximal femoral trabecular structure revealed significant preservation of apparent BV/TV, apparent trabecular number, and apparent trabecular spacing in post-menopausal women treated with calcitonin compared to a placebo group at 2 years [55]. Over the same time, no significant change in DXA BMD was observed helping to explain an earlier study showing substantial reduction in fracture risk with calcitonin despite only a small increase in BMD [55, 56].

As well as analyzing the trabecular component of bone, MR imaging has also been applied to the study of the bone cortex. The amount of trabecular or cortical bone varies considerably with cortical bone only accounting for 10 % of vertebral body bone though 75 % of femoral neck bone and 50 % of femoral inter-trochanteric bone [57]. As the cortex looses bone, it becomes thinner and more porous. Cortical porosity is a challenging parameter to measure in vivo [58]. However, MRI allows a different approach in that ultrashort echo-time imaging can quantify cortical bone water content and one may be able to use cortical water content as a surrogate marker of cortical porosity [59]. Tibial cortical water content in patients with end-stage chronic renal failure was found to be 135 % higher than in pre-menopausal women and 43 % higher than in post-menopausal women although no difference in cortical BMD was found between the three groups indicating how cortical water content may prove to be a better indicator of cortical bone loss and cortical porosity than cortical BMD [59].

MR also has the capability of assessing marrow fat content, molecular diffusion, and marrow perfusion. Although an inverse relationship between increasing marrow fat and trabecular bone loss in senile osteoporosis has been long recognized, several recent findings have changed the perception that marrow fat was simply a metabolically inactive tissue filling the void vacated by trabecular bone [60, 61]. First, marrow fat, haematopoetic marrow, and trabecular bone mass are inextricably linked through differentiation of a pluripotent mesenchymal stem cell which has the ability to differentiate along adipocytic, haematopoetic, and osteocytic cell lines [62]. Second, marrow adipocytes have been shown to be both potentially self-promotive and metabolically active with existing adipocytes inducing differentiation of further adipocytes while actively suppressing osteoblastogenesis [63–66]. It is conceivable, therefore, that marrow fat may be, at least in part, driving bone loss and contributing to osteoporosis [65, 66]. Marrow fat content increases sharply in female subjects between 55 and 65 years of age, while male subjects continue to increase marrow fat at a more gradual steady

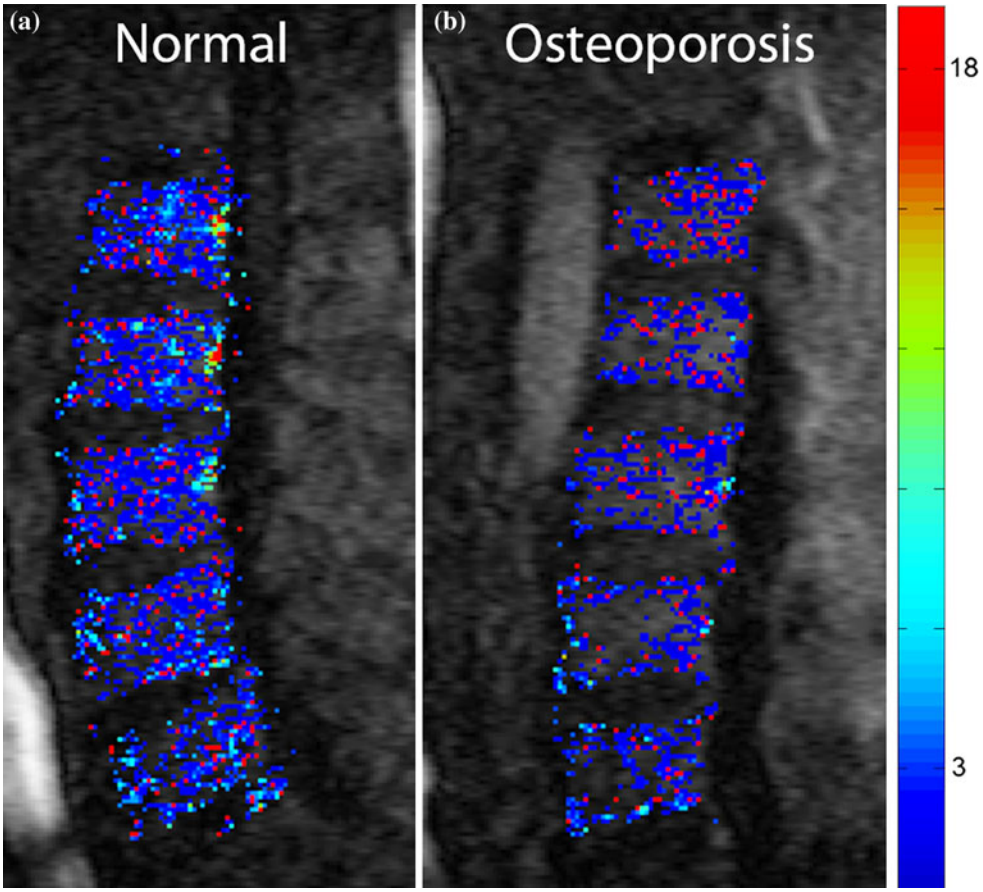

Fig. 5 Color map representation of pharmacokinetic modeling (amplitude map) of lumbar vertebral bone marrow perfusion in subjects with **a** normal bone density and **b** osteoporosis. Bone marrow perfusion is significantly reduced in subjects with osteoporosis compared to those with normal BMD

rate. This increased deposition in marrow fat concurs with recognized changes in extraosseous fat distribution in postmenopausal females [67, 68].

MRI studies have shown how perfusion is reduced in non-fractured osteoporotic vertebrae bodies compared to those of normal BMD [69, 70] (Fig. 5). Good bone perfusion is clearly a pre-requisite for normal bone metabolism and fracture healing, including microdamage repair. MR perfusion studies how the femoral head and trochanteric region of the proximal femur are normally poorly perfused compared to the femoral neck and shaft region [71]. All hip perfusion parameters decrease as BMD decreases though particularly in the femoral neck region, the most common site of proximal femoral fracture [71, 72]. Compared to normal BMD subjects, perfusion parameters in the femoral neck region reduced by approx. 40–60 % in the femoral neck region in osteoporotic subjects compared to normal BMD subjects [72]. Additional recently developed MR applications show the possibility of quantifying the amount of collagen matrix in bone using specifically designed WASPI pulse sequences [73] while phosphorus spectroscopy (^{31}PMRS) can be used to measure the mineralized phosphorus component. Combining these techniques allows the possibility of measuring "bone matrix mineralization" and potentially differentiating between osteoporosis and osteomalacia [74, 75].

Advances in imaging complications of osteoporosis

The overriding complication of osteoporosis is insufficiency fracture. All of the work put into understanding, screening, diagnosing, and treating osteoporosis is designed with one aim in mind—to prevent osteoporotic fracture. An insufficiency fracture is a fracture occurring under normal physiological loads. In other words, a fracture occurring from circumstances which would not normally be expected to result in fracture. Insufficiency fractures most commonly involve the vertebral bodies, proximal femora, distal radius, sacrum, and pubic bones and less commonly, the proximal tibiae, the calcaneum, sacrum, and ribs. These bones are particularly prone to insufficiency fracture as they have a greater dependence on

trabecular bone for their strength (such as the vertebral body) or they are located in areas where physical stress is concentrated ("stress riser"). Insufficiency fractures differ from standard traumatic fractures in that they are often incremental in nature progressing over weeks or months rather than occurring as a one-off, all or nothing, event.

Insufficiency fractures are important to recognize since they provide indisputable evidence of reduced bone strength. The easily applicable DXA *T*-score criteria for diagnosing osteoporosis have become so entrenched into clinical practice that the significance of insufficiency fracture has been somewhat undervalued [76]. The presence of an insufficiency fracture overrides any information from DXA examination with regard to the presence of osteoporosis. For example, it is not correct to say that, in the absence of other bone disorder, that a patient with an insufficiency fracture does not have osteoporosis "as the DXA *T*-score is >-2.5". For this reason, the National Osteoporosis Foundation has recommended that patients aged over 50 years with non-traumatic new vertebral fracture receive appropriate bone protective/bone enhancing therapy, irrespective of DXA *T*-score [77]. One should, however, not have to wait for an insufficiency fracture to occur before diagnosing osteoporosis and hence the ongoing quest to identify the osteoporotic process before insufficiency fracture occurs.

Most insufficiency fractures are readily visible radiographically at the time of clinical presentation. However, since these fractures may primarily involve trabecular bone and since trabecular bone is not easily assessed on radiographs or CT, particularly when rarefied in osteoporosis, insufficiency fractures may not always be visible radiographically [78]. MRI has revolutionized clinical practice regarding the recognition and characterization of

Fig. 6 **a** Radiograph and **b** CT of proximal femur show osteopenia but no fracture in elderly patient with clinically suspected proximal femoral fracture. **c** T1-weighted and **d** T2-weighted fat-suppressed image clearly shows a fracture line extending along most the intertrochanteric area. This was successfully treated with screw fixation

insufficiency fractures leading to increased awareness of this entity among health care professionals. The hallmarks of an insufficiency fracture on MRI are localized bone marrow edema usually, though not invariably, accompanied by a hypointense linear fracture line.

The vast majority of vertebral fractures are detected with radiography though increasingly these fractures are being identified using VXA by DXA and on CT examinations performed for thoraco-abdominal indications [79]. MRI allows detection of vertebral or other insufficiency fracture at a very early stage, enables determination of fracture age, and distinction between osteoporotic and neoplastic fracture with greater sensitivity than other imaging techniques [80]. Conversely, a normal MRI fully excludes the presence of an insufficiency fracture. MR-based perfusion parameters are reduced in osteoporotic vertebral fractures compared to adjacent non-fractured vertebrae [81]. The smaller the enhancement area within an acutely fractured vertebral body, the more likely it will lose height on subsequent follow-up [82]. MRI may also have the potential to predict non-union which occurs in about 10 % of osteoporotic vertebral fractures and is associated with more severe back pain than united fractures [83]. It is feasible that these particular types of fracture may benefit from pro-active fracture treatment such as vertebroplasty.

About 10 % of osteoporotic neck of femur fractures are radiographically occult [84]. Similarly, other fractures around the pelvis (acetabulum, pubic rami, sacrum), joint pathology or soft tissue injury can masquerade clinically as a proximal femoral fracture. MRI will consistently demonstrate fractures in approx. 40 % of those patients with clinically suspected neck of femur fracture though no fracture visible on radiographs [85] and is more sensitive than CT or bone scintigraphy is this respect [86] (Fig. 6). The MR protocol used is straightforward making it relatively easy to schedule these examinations within 24 h of admission [87]. Previously, these patients would have been discharged from hospital only to return in 1–2 weeks with a displaced neck of femur fracture [84]. In those cases in whom MRI does not reveal a neck of femur fracture, MRI

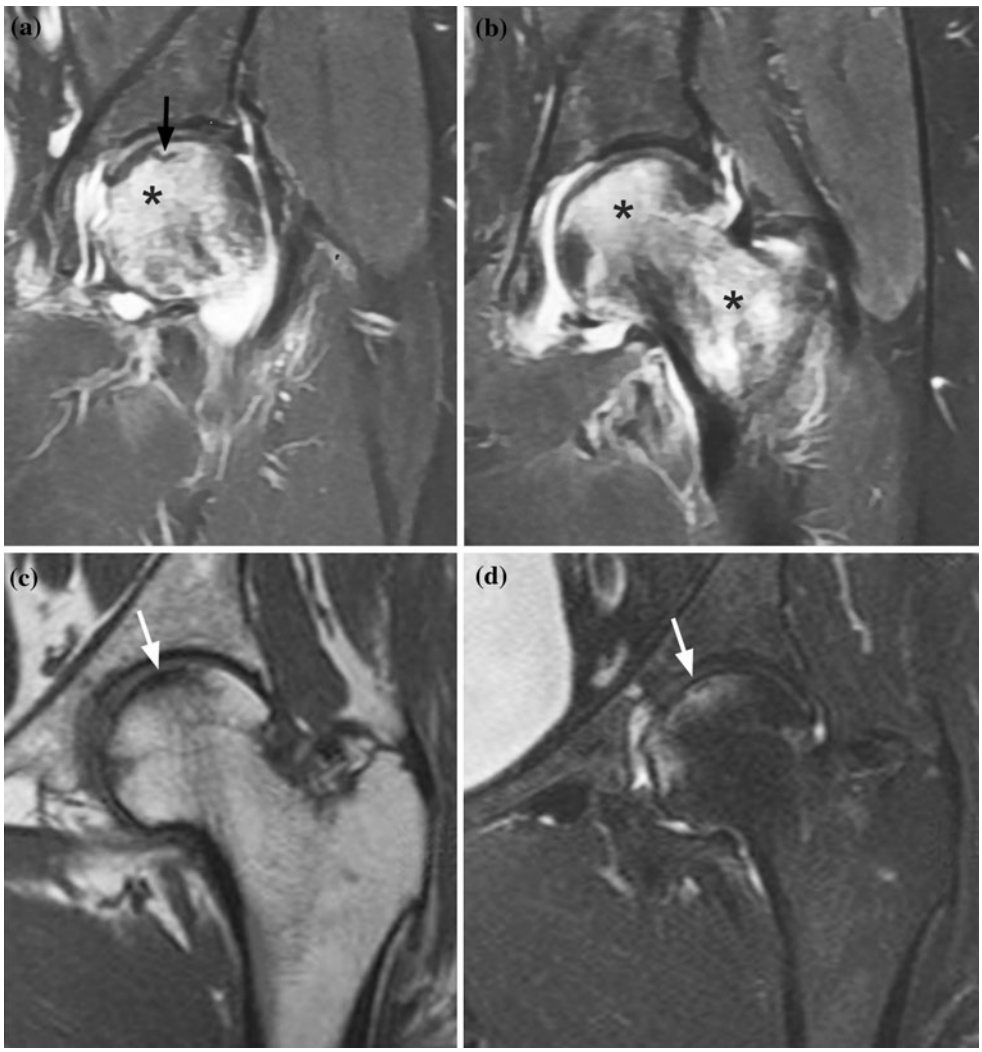

Fig. 7 **a** T2-weighted fat-suppressed oblique coronal MR images in elderly patient with recent onset of hip pain show subchondral fracture of femoral head (*arrow*) and **b** diffuse marrow edema of proximal femur (*asterisk*). Radiograph (not shown) revealed osteopenia but no fracture. **c** T1-weighted and **d** fat-suppressed MR oblique coronal MR image after 6 weeks of limited weight bearing show persistence of subchondral fracture (*arrows*) though resolution of marrow edema consistent with healing response

Fig. 8 Axial CT showing insufficiency fracture of both sacral ala (*arrows*) on background of osteoporotic bone

will usually demonstrate other pelvic fractures (acetabular, pubic rami or sacrum) or injury (such as osteonecrosis, hematoma, muscle or tendon injury) to account for symptoms [85, 87]. MRI is also beneficial in patients whom fractures seem confined to the greater trochanter on radiographs as the majority will be seen on MRI to have inter-trochanteric fracture extension necessitating surgical fixation [88].

A less frequently seen complication of osteoporosis is subchondral insufficiency fracture of the femoral head or proximal tibia [89]. These fractures are usually radiographically occult though can be readily seen on MRI as a serpiginous thin T1-hypointense line convex to the femoral head articular surface [90] (Fig. 7). This line represents the fracture line surrounded by granulation tissue and marrow edema and will enhance on MRI [91]. Early recognition of these fractures by MRI is important since non-weight bearing can lead to alleviation of symptoms. Conversely, failure to recognize and treat these subchondral insufficiency fractures may result in them progressing to rapid dissolution of the femoral head or tibial condyle [92].

Sacral insufficiency fractures are a quite common cause of debilitating back pain in the elderly, often associated with a delay in diagnosis since symptoms mimic those of degenerative disk disease or radiculopathy. Most are not visible radiographically [93, 94] though bone scintigraphy, CT or MRI can detect and classify these fracture with high specificity [86, 94] (Fig. 8). Fracture line orientation, which is typically vertical along the sacral ala with an occasional horizontal component is best depicted by CT. CT can also determine fracture healing and, in the research setting, FEA assessment [94] (Fig. 9). Sacroplasty with injection of bone cement into the fracture line under image guidance has recently been introduced as a means to treat sacral insufficiency fracture, though is probably best reserved for those fractures not responding to conservative treatment. One problem with sacroplasty, which also

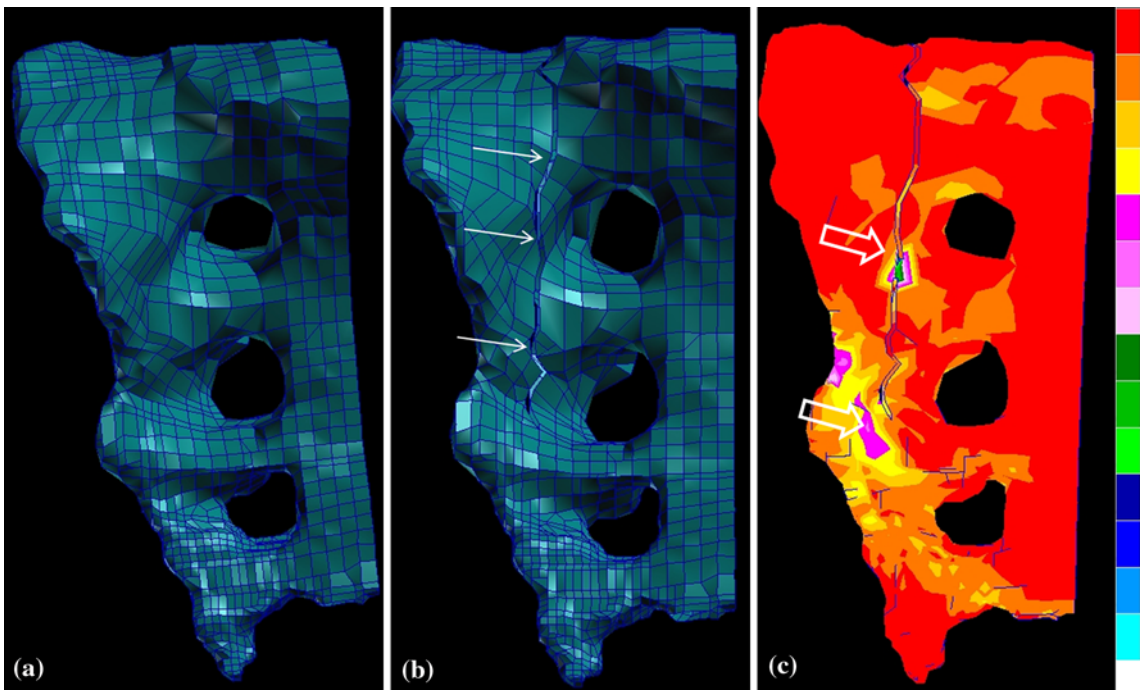

Fig. 9 Finite element model of hemisacrum constructed from cadaveric CT data in patient with **a** normal sacrum and **b** fractured sacrum. The *arrow* in Fig. 9b represents the fracture propagation line. **c** After simulated application of a 35 kg load, the stress (kPa) concentration around the fracture line, especially distally can be appreciated (*open arrows*). (Courtesy of Pearse Morris)

applies to vertebroplasty, is that these processes interfere with normal fracture healing.

In conclusion, one can appreciate the tremendous advances made over the past two decades in assessing osteoporosis and its complications. High resolution imaging combined with sophisticated computational techniques can now directly predict bone strength and provide a detailed analysis of bone structure. Yet limitations peculiar to each of these techniques currently hinder adoption into mainstream clinical practice. The ultimate quest for bone quality imaging remains an available, safe, high resolution technique capable of fully predicting bone strength, capable of showing how bone strength is faltering and precisely monitoring treatment effect. Whether this technique will be based on acquisition of spine/hip data or reflective peripheral data is still not clear. When such a technique evolves, alongside the possibility of mechanistic-specific treatment options, the occurrence of debilitating insufficiency fracture in the middle-aged and elderly will considerably lessen. In the meantime, mainstream imaging will continue to enhance the detection of insufficiency fracture, though until then, we should all be aiming to improve general awareness of this fracture type as a marker of severely impaired bone strength.

References

1. G. Mazziotti, J. Bilezikian, E. Canalis, D. Cocchi, A. Giustina, New understanding and treatments for osteoporosis. Endocrine **41**, 58–69 (2012)
2. J. Compston, The use of combination therapy in the treatment of postmenopausal osteoporosis. Endocrine **41**, 11–18 (2012)
3. World Health Organisation, Assessment of fracture risk and its implication to screening for postmenopausal osteoporosis. World Health Organ. Tech. Rep. Ser. **843**, 1–129 (1994)
4. H.S. Lynn, E.M. Lau, B. Au, P.C. Leung, Bone mineral density reference norms for Hong Kong Chinese. Osteoporos. Int. **16**, 1663–1668 (2005)
5. E.W. Yu, B.J. Thomas, J.K. Brown, J.S. Finkelstein, Simulated increases in body fat and errors in bone mineral density measurements by DXA and QCT. J. Bone Miner. Res. (2011). doi: 10.1002/jbmr.506
6. G.M. Blake, J.F. Griffith, D.K. Yeung, P.C. Leung, I. Fogelman, Effect of increasing vertebral marrow fat content on BMD measurement, *T*-score status and fracture risk prediction by DXA. Bone **44**, 495–501 (2009)
7. D. Marshall, O. Johnell, H. Wedel, Meta-analysis of how well measures of bone mineral density predict occurrence of osteoporotic fractures. BMJ **312**, 1254–1259 (1996)
8. J.A. Kanis, An update on the diagnosis of osteoporosis. Curr. Rheumatol. Rep. **2**, 62–66 (2000)
9. NIH Consensus Development Panel on Osteoporosis Prevention, Diagnosis, and Therapy, Osteoporosis prevention, diagnosis, and therapy. JAMA **285**, 785–795 (2001)
10. E. Sornay-Rendu, F. Munoz, P. Garnero, F. Duboeuf, P.D. Delmas, Identification of osteopenic women at high risk of fracture: the OFELY study. J. Bone Miner. Res. **20**, 1813–1819 (2005)
11. S.C. Schuit, M. van der Klift, A.E. Weel, C.E. de Laet, H. Burger, E. Seeman, A. Hofman, A.G. Uitterlinden, J.P. van Leeuwen, H.A. Pols, Fracture incidence and association with bone mineral density in elderly men and women: the Rotterdam Study. Bone **38**, 603 (2006)
12. S.R. Cummings, D.B. Karpf, F. Harris, H.K. Genant, K. Ensrud, A.Z. LaCroix, D.M. Black, Improvement in spine bone density and reduction in risk of vertebral fractures during treatment with antiresorptive drugs. Am. J. Med. **112**, 281–289 (2002)
13. P.D. Delmas, Z. Li, C. Cooper, Relationship between changes in bone mineral density and fracture risk reduction with antiresorptive drugs: some issues with meta-analyses. J. Bone Miner. Res. **19**, 330–337 (2004)
14. J.T. Schousboe, T. Vokes, S.B. Broy, L. Ferrar, F. McKiernan, C. Roux, N. Binkley, Vertebral fracture assessment: the 2007 ISCD official positions. J. Clin. Densitom. **11**, 92–108 (2008)
15. J.A. Kanis, O. Johnell, A. Oden, H. Johansson, E. McCloskey, FRAX and the assessment of fracture probability in men and women from the UK. Osteoporos. Int. **19**, 385–397 (2008)
16. A.S. Karlamangla, E. Barrett-Connor, J. Young, G.A. Greendale, Hip fracture risk assessment using composite indices of femoral neck strength: the Rancho Bernardo study. Osteoporos. Int. **15**, 62–70 (2004)
17. N. Yu, Y.J. Liu, Y. Pei, L. Zhang, S. Lei, N.R. Kothari, D.Y. Li, C.J. Papasian, J. Hamilton, J.Q. Cai, H.W. Deng, Evaluation of compressive strength index of the femoral neck in Caucasians and Chinese. Calcif. Tissue Int. **87**, 324–332 (2010)
18. K.G. Faulkner, W.K. Wacker, H.S. Barden, C. Simonelli, P.K. Burke, S. Ragi, L. Del Rio, Femur strength index predicts hip fracture independent of bone density and hip axis length. Osteoporos. Int. **17**, 593–599 (2006)
19. S. Ishii, J.A. Cauley, C.J. Crandall, P. Srikanthan, G.A. Greendale, M.H. Huang, M.E. Danielson, A.S. Karlamangla, Diabetes and femoral neck strength: findings from the hip strength across the menopausal transition study. J. Clin. Endocrinol. Metab. **97**, 190–197 (2012)
20. S. Kolta, A. Le Bras, D. Mitton, V. Bousson, J.A. de Guise, J. Fechtenbaum, J.D. Laredo, C. Roux, W. Skalli, Three-dimensional X-ray absorptiometry (3D-XA): a method for reconstruction of human bones using a dual X-ray absorptiometry device. Osteoporos. Int. **16**, 969–976 (2005)
21. A. Le Bras, S. Kolta, P. Soubrane, W. Skalli, C. Roux, D. Mitton, Assessment of femoral neck strength by 3-dimensional X-ray absorptiometry. J. Clin. Densitom. **9**, 425–430 (2006)
22. O. Ahmad, K. Ramamurthi, K.E. Wilson, K. Engelke, R.L. Prince, R.H. Taylor, Volumetric DXA (VXA): a new method to extract 3D information from multiple in vivo DXA images. J. Bone Miner. Res. **25**, 2744–2751 (2011). Erratum in: J. Bone Miner. Res. 26, 439 (2011)
23. A. Andreoli, A. De Lorenzo, F. Cadeddu, L. Iacopino, M. Grande, New trends in nutritional status assessment of cancer patients. Eur. Rev. Med. Pharmacol. Sci. **15**, 469–480 (2011)
24. Bazzocchi A, Ciccarese F, Diano D, Spinnato P, Albisinni U, Rossi C, Guglielmi G. Dual-Energy X-ray Absorptiometry in the Evaluation of Abdominal Aortic Calcifications J. Clin. Densitom. **15**, 198–204 (2012)
25. J.F. Griffith, S.M. Kumta, Y. Huang, Hard arteries, weak bones. Skeletal Radiol. **40**, 517–521 (2011)
26. H.K. Genant, K. Engelke, S. Prevrhal, Advanced CT bone imaging in osteoporosis. Rheumatology (Oxford) **47,** iv9–16 (2008)
27. E. Seeman, The structural basis of bone fragility in men. Bone **25**, 143–147 (1999)
28. Y. Duan, X.F. Wang, A. Evans, E. Seeman, Structural and biomechanical basis of racial and sex differences in vertebral fragility in Chinese and Caucasians. Bone **36**, 987–998 (2005)

29. M.L. Bouxsein, E. Seeman, Quantifying the material and structural determinants of bone strength. Best Pract. Res. Clin. Rheumatol. **23**, 741–753 (2009)
30. B.L. Riggs, L.J. Melton 3rd, R.A. Robb, J.J. Camp, E.J. Atkinson, J.M. Peterson, P.A. Rouleau, C.H. McCollough, M.L. Bouxsein, S. Khosla, Population-based study of age and sex differences in bone volumetric density, size, geometry, and structure at different skeletal sites. J. Bone Miner. Res. **19**, 1945–1954 (2004)
31. H.K. Genant, M. Jergas, L. Palermo, M. Nevitt, R.S. Valentin, D. Black, S.R. Cummings, Comparison of semiquantitative visual and quantitative morphornetric assessment of prevalent and incident vertebral fractures in osteoporosis The Study of Osteoporotic Fractures Research Group. J. Bone Miner. Res. **11**, 984–996 (1996)
32. X. Banse, J.P. Devogelaer, M. Grynpas, Patient-specific microarchitecture of vertebral cancellous bone: a peripheral quantitative computed tomographic and histological study. Bone **30**, 829–835 (2002)
33. B.A. Christiansen, M.L. Bouxsein, Biomechanics of vertebral fractures and the vertebral fracture cascade. Curr. Osteoporos. Rep. **8**, 198–204 (2010)
34. A.J. Fields, G.L. Lee, X.S. Liu, M.G. Jekir, X.E. Guo, T.M. Keaveny, Influence of vertical trabeculae on the compressive strength of the human vertebra. J. Bone Miner. Res. **26**, 263–269 (2011)
35. J.S. Thomsen, E.N. Ebbesen, L.I. Mosekilde, Age-related differences between thinning of horizontal and vertical trabeculae in human lumbar bone as assessed by a new computerized method. Bone **31**, 136–142 (2002)
36. X. Shi, X.S. Liu, X. Wang, X.E. Guo, G.L. Niebur, Effects of trabecular type and orientation on microdamage susceptibility in trabecular bone. Bone **46**, 1260–1266 (2010)
37. P. Mc Donnell, N. Harrison, M.A. Liebschner, P.E. Mc Hugh, Simulation of vertebral trabecular bone loss using voxel finite element analysis. J. Biomech. **42**, 2789–2796 (2009)
38. T.M. Keaveny, Biomechanical computed tomography—noninvasive bone strength analysis using clinical computed tomography scans. Ann. N. Y. Acad. Sci. **1192**, 57–65 (2010)
39. B.A. Christiansen, D.L. Kopperdahl, D.P. Kiel, T.M. Keaveny, M.L. Bouxsein, Mechanical contributions of the cortical and trabecular compartments contribute to differences in age-related changes in vertebral body strength in men and women assessed by QCT-based finite element analysis. J. Bone Miner. Res. **26**, 974–983 (2011)
40. K.M. Kim, J.K. Brown, K.J. Kim, H.S. Choi, H.N. Kim, Y. Rhee, S.K. Lim, Differences in femoral neck geometry associated with age and ethnicity. Osteoporos. Int. **22**, 2165–2174 (2011)
41. R.D. Carpenter, S. Sigurdsson, S. Zhao, Y. Lu, G. Eiriksdottir, G. Sigurdsson, B.Y. Jonsson, S. Prevrhal, T.B. Harris, K. Siggeirsdottir, V. Guðnason, T.F. Lang, Effects of age and sex on the strength and cortical thickness of the femoral neck. Bone **48**, 741–747 (2011)
42. S. Amin, D.L. Kopperdhal, L.J. Melton 3rd, S.J. Achenbach, T.M. Therneau, B.L. Riggs, T.M. Keaveny, S. Khosla, Association of hip strength estimates by finite-element analysis with fractures in women and men. J. Bone Miner. Res. **26**, 1593–1600 (2011)
43. T.M. Keaveny, D.L. Kopperdahl, L.J. Melton 3rd, P.F. Hoffmann, S. Amin, B.L. Riggs, S. Khosla, Age-dependence of femoral strength in white women and men. J. Bone Miner. Res. **25**, 994–1001 (2010)
44. C. Graeff, Y. Chevalier, M. Charlebois, P. Varga, D. Pahr, T.N. Nickelsen, M.M. Morlock, C.C. Glüer, P.K. Zysset, Improvements in vertebral body strength under teriparatide treatment assessed in vivo by finite element analysis: results from the EUROFORS study. J. Bone Miner. Res. **24**, 1672–1680 (2009)
45. Y. Kang, K. Engelke, C. Fuchs, W.A. Kalender, An anatomic coordinate system of the femoral neck for highly reproducible BMD measurements using 3D QCT. Comput. Med. Imaging Graph **29**, 533–541 (2005)
46. K. Engelke, A. Mastmeyer, V. Bousson, T. Fuerst, J.D. Laredo, W.A. Kalender, Reanalysis precision of 3D quantitative computed tomography (QCT) of the spine. Bone **44**, 566–572 (2009)
47. K. Engelke, T. Fuerst, G. Dasic, R.Y. Davies, H.K. Genant, Regional distribution of spine and hip QCT BMD responses after one year of once-monthly ibandronate in postmenopausal osteoporosis. Bone **46**, 1626–1632 (2010)
48. X.S. Liu, A. Cohen, E. Shane, P.T. Yin, E.M. Stein, H. Rogers, S.L. Kokolus, D.J. McMahon, J.M. Lappe, R.R. Recker, T. Lang, X.E. Guo, Bone density, geometry, microstructure, and stiffness: Relationships between peripheral and central skeletal sites assessed by DXA, HR-pQCT, and cQCT in premenopausal women. J. Bone Miner. Res. **25**, 2229–2238 (2010)
49. S. Khosla, B.L. Riggs, E.J. Atkinson, A.L. Oberg, L.J. McDaniel, M. Holets, J.M. Peterson, L.J. Melton 3rd, Effects of sex and age on bone microstructure at the ultradistal radius: a population-based noninvasive in vivo assessment. J. Bone Miner. Res. **21**, 124–131 (2006)
50. B.L. Riggs, L.J. Melton, R.A. Robb, J.J. Camp, E.J. Atkinson, L. McDaniel, S. Amin, P.A. Rouleau, S. Khosla, A population-based assessment of rates of bone loss at multiple skeletal sites: evidence for substantial trabecular bone loss in young adult women and men. J. Bone Miner. Res. **23**, 205–214 (2008)
51. E. Seeman, P.D. Delmas, D.A. Hanley, D. Sellmeyer, A.M. Cheung, E. Shane, A. Kearns, T. Thomas, S.K. Boyd, S. Boutroy, C. Bogado, S. Majumdar, M. Fan, C. Libanati, J. Zanchetta, Microarchitectural deterioration of cortical and trabecular bone: differing effects of denosumab and alendronate. J. Bone Miner. Res. **25**, 1886–1894 (2010)
52. R. Krug, J. Carballido-Gamio, A.J. Burghardt, G. Kazakia, B.H. Hyun, B. Jobke, S. Banerjee, M. Huber, T.M. Link, S. Majumdar, Assessment of trabecular bone structure comparing magnetic resonance imaging at 3 Tesla with high-resolution peripheral quantitative computed tomography ex vivo and in vivo. Osteoporos. Int. **19**, 653–661 (2008)
53. F.W. Wehrli, M.B. Leonard, P.K. Saha, B.R. Gomberg, Quantitative high-resolution magnetic resonance imaging reveals structural implications of renal osteodystrophy on trabecular and cortical bone. J. Magn. Reson. Imaging **20**, 83–89 (2004)
54. R. Krug, S. Banerjee, E.T. Han, D.C. Newitt, T.M. Link, S. Majumdar, Feasibility of in vivo structural analysis of high-resolution magnetic resonance images of the proximal femur. Osteoporos. Int. **16**, 1307–1314 (2005). Erratum in: Osteoporos. Int. **17,** 1705 (2006)
55. C.H. Chesnut 3rd, S. Majumdar, D.C. Newitt, A. Shields, J. Van Pelt, E. Laschansky, M. Azria, A. Kriegman, M. Olson, E.F. Eriksen, L. Mindeholm, Effects of salmon calcitonin on trabecular microarchitecture as determined by magnetic resonance imaging: results from the QUEST study. J. Bone Miner. Res. **20**, 1548–1561 (2005)
56. C.H. Chesnut 3rd, S. Silverman, K. Andriano, H. Genant, A. Gimona, S. Harris, D. Kiel, M. LeBoff, M. Maricic, P. Miller, C. Moniz, M. Peacock, P. Richardson, N. Watts, D. Baylink, A randomized trial of nasal spray salmon calcitonin in postmenopausal women with established osteoporosis: the prevent recurrence of osteoporotic fractures study. PROOF Study Group. Am. J. Med. **109**, 267–276 (2000)
57. R. Krug, A.J. Burghardt, S. Majumdar, T.M. Link, High-resolution imaging techniques for the assessment of osteoporosis. Radiol. Clin. North Am. **48**, 601–621 (2010)
58. V. Bousson, C. Bergot, A. Meunier, F. Barbot, C. Parlier-Cuau, A.M. Laval-Jeantet, J.D. Laredo, CT of the middiaphyseal femur:

cortical bone mineral density and relation to porosity. Radiology **217**, 179–187 (2000)
59. A. Techawiboonwong, H.K. Song, M.B. Leonard, F.W. Wehrli, Cortical bone water: in vivo quantification with ultrashort echo-time MR imaging. Radiology **248**, 824–833 (2008)
60. P. Meunier, J. Aaron, C. Edouard, G. Vignon, Osteoporosis and the replacement of cell populations of the marrow by adipose tissue. A quantitative study of 84 iliac bone biopsies. Clin. Orthop. Relat. Res. **80**, 147–154 (1971)
61. J.M. Gimble, C.E. Robinson, X. Wu, K.A. Kelly, The function of adipocytes in the bone marrow stroma: an update. Bone **19**, 421–428 (1996)
62. M.F. Pittenger, A.M. Mackay, S.C. Beck, R.K. Jaiswal, R. Douglas, J.D. Mosca, M.A. Moorman, D.W. Simonetti, S. Craig, D.R. Marshak, Multilineage potential of adult human mesenchymal stem cells. Science **284**, 143–147 (1999)
63. B. Lecka-Czernik, E.J. Moerman, D.F. Grant, J.M. Lehmann, S.C. Manolagas, R.L. Jilka, Divergent effects of selective peroxisome proliferator-activated receptor-gamma 2 ligands on adipocyte versus osteoblast differentiation. Endocrinology **143**, 2376–2384 (2002)
64. J.M. Gimble, M.E. Nuttall, Bone and fat: old questions, new insights. Endocrine **23**, 183–188 (2004)
65. G. Duque, Bone and fat connection in aging bone. Curr. Opin. Rheumatol. **20**, 429–434 (2008)
66. C.J. Rosen, C. Ackert-Bicknell, J.P. Rodriguez, A.M. Pino, Marrow fat and the bone microenvironment: developmental, functional, and pathological implications. Crit. Rev. Eukaryot. Gene Expr. **19**, 109–124 (2009)
67. M.J. Toth, A. Tchernof, C.K. Sites, E.T. Poehlman, Menopause-related changes in body fat distribution. Ann. N. Y. Acad. Sci. **904**, 502–506 (2000)
68. K. Blouin, A. Boivin, A. Tchernof, Androgens and body fat distribution. J. Steroid Biochem. Mol. Biol. **108**, 272–280 (2008)
69. J.F. Griffith, D.K. Yeung, G.E. Antonio, F.K. Lee, A.W. Hong, S.Y. Wong, E.M. Lau, P.C. Leung, Vertebral bone mineral density, marrow perfusion, and fat content in healthy men and men with osteoporosis: dynamic contrast-enhanced MR imaging and MR spectroscopy. Radiology **236**, 945–951 (2005)
70. J.F. Griffith, D.K. Yeung, G.E. Antonio, S.Y. Wong, T.C. Kwok, J. Woo, P.C. Leung, Vertebral marrow fat content and diffusion and perfusion indexes in women with varying bone density: MR evaluation. Radiology **241**, 831–838 (2006)
71. J.F. Griffith, D.K. Yeung, P.H. Tsang, K.C. Choi, T.C. Kwok, A.T. Ahuja, K.S. Leung, P.C. Leung, Compromised bone marrow perfusion in osteoporosis. J. Bone Miner. Res. **23**, 1068–1075 (2008)
72. Y.X. Wang, J.F. Griffith, A.W. Kwok, J.C. Leung, D.K. Yeung, A.T. Ahuja, P.C. Leun, Reduced bone perfusion in proximal femur of subjects with decreased bone mineral density preferentially affects the femoral neck. Bone **45**, 711–715 (2009)
73. H. Cao, J.L. Ackerman, M.I. Hrovat, L. Graham, M.J. Glimcher, Y. Wu, Quantitative bone matrix density measurement by water- and fat-suppressed proton projection MRI (WASPI) with polymer calibration phantoms. Magn. Reson. Med. **60**, 1433–1443 (2008)
74. H. Cao, A. Nazarian, J.L. Ackerman, B.D. Snyder, A.E. Rosenberg, R.M. Nazarian, M.I. Hrovat, G. Dai, D. Mintzopoulos, Y. Wu, Quantitative (31)P NMR spectroscopy and (1)H MRI measurements of bone mineral and matrix density differentiate metabolic bone diseases in rat models. Bone **46**, 1582–1590 (2010)
75. Y. Wu, M.I. Hrovat, J.L. Ackerman, T.G. Reese, H. Cao, K. Ecklund, M.J. Glimcher, Bone matrix imaged in vivo by water- and fat-suppressed proton projection MRI (WASPI) of animal and human subjects. J. Magn. Reson. Imaging **31**, 954–963 (2010)
76. P.D. Delmas, L. van de Langerijt, N.B. Watts, R. Eastell, H. Genant, A. Grauer, D.L. Cahall, IMPACT Study Group, underdiagnosis of vertebral fractures is a worldwide problem: the IMPACT study. J. Bone Miner. Res. **20**, 557–563 (2005)
77. National Osteoporosis Foundation, The Clinician's Guide to Prevention and Treatment of Osteoporosis. National Osteoporosis Foundation. Washington, DC, USA. (2010) [http://www.nof.org/sites/default/files/pdfs/NOF_ClinicianGuide2009_v7.pdf]
78. C.R. Krestan, U. Nemec, S. Nemec, Imaging of insufficiency fractures. Semin. Musculoskelet. Radiol. **15**, 198–207 (2011)
79. A.L. Williams, A. Al-Busaidi, P.J. Sparrow, J.E. Adams, R.W. Whitehouse, Under-reporting of osteoporotic vertebral fractures on computed tomography. Eur. J. Radiol. **69**, 179–183 (2009)
80. J.F. Griffith, G. Guglielmi, Vertebral fracture. Radiol. Clin. North Am. **48**, 519–529 (2010)
81. A. Biffar, G.P. Schmidt, S. Sourbron, M. D'Anastasi, O. Dietrich, M. Notohamiprodjo, M.F. Reiser, A. Baur-Melnyk, Quantitative analysis of vertebral bone marrow perfusion using dynamic contrast-enhanced MRI: initial results in osteoporotic patients with acute vertebral fracture. J. Magn. Reson. Imaging **33**, 676–683 (2011)
82. T. Kanchiku, T. Taguchi, K. Toyoda, K. Fujii, S. Kawai, Dynamic contrast-enhanced magnetic resonance imaging of osteoporotic vertebral fracture. Spine **28**, 2522–2526 (2003)
83. T. Tsujio, H. Nakamura, H. Terai, M. Hoshino, T. Namikawa, A. Matsumura, M. Kato, A. Suzuki, K. Takayama, W. Fukushima, K. Kondo, Y. Hirota, K. Takaoka, Characteristic radiographic or magnetic resonance images of fresh osteoporotic vertebral fractures predicting potential risk for nonunion: a prospective multicenter study. Spine **36**, 1229–1235 (2011)
84. G. Pathak, M.J. Parker, G.A. Pryor, Delayed diagnosis of femoral neck fractures. Injury **28**, 299–301 (1997)
85. H.A. Chatha, S. Ullah, Z.Z. Cheema, Review article: Magnetic resonance imaging and computed tomography in the diagnosis of occult proximal femur fractures. J. Orthop. Surg. (Hong Kong) **19**, 99–103 (2011)
86. M.C. Cabarrus, A. Ambekar, Y. Lu, T.M. Link, MRI and CT of insufficiency fractures of the pelvis and the proximal femur. AJR Am. J. Roentgenol. **191**, 995–1001 (2008)
87. Y.P. Lee, J.F. Griffith, G.E. Antonio, N. Tang, K.S. Leung, Early magnetic resonance imaging of radiographically occult osteoporotic fractures of the femoral neck. Hong Kong Med. J. **10**, 271–275 (2004)
88. J.G. Craig, B.R. Moed, W.R. Eyler, M. van Holsbeeck, Fractures of the greater trochanter: intertrochanteric extension shown by MR imaging. Skeletal Radiol. **29**, 572–576 (2000)
89. T. Yamamoto, Y. Iwamoto, R. Schneider, P.G. Bullough, Histopathological prevalence of subchondral insufficiency fracture of the femoral head. Ann. Rheum. Dis. **67**, 150–153 (2008)
90. G. Zhao, T. Yamamoto, S. Ikemura, Y. Nakashima, T. Mawatari, G. Motomura, Y. Iwamoto, A histopathological evaluation of a concave-shaped low-intensity band on T1-weighted MR images in a subchondral insufficiency fracture of the femoral head. Skeletal Radiol. **39**, 185–188 (2010)
91. K. Miyanishi, T. Hara, S. Kaminomachi, H. Maeda, H. Watanabe, T. Torisu, Contrast-enhanced MR imaging of subchondral insufficiency fracture of the femoral head: a preliminary comparison with that of osteonecrosis of the femoral head. Arch. Orthop. Trauma Surg. **129**, 583–589 (2009)
92. T. Yamamoto, K. Takabatake, Y. Iwamoto, Subchondral insufficiency fracture of the femoral head resulting in rapid destruction of the hip joint: a sequential radiographic study. AJR Am. J. Roentgenol. **178**, 435–437 (2002)
93. R. Schneider, J. Yacovone, B. Ghelman, Unsuspected sacral fractures: detection by radionuclide bone scanning. AJR Am. J. Roentgenol. **144**, 337–341 (1985)
94. E.M. Lyders, C.T. Whitlow, M.D. Baker, P.P. Morris, Imaging and treatment of sacral insufficiency fractures. AJNR Am. J. Neuroradiol. **31**, 201–210 (2010)